



Mateus Lenz Leite (Autor)

# In situ generated $\beta\text{-Yb}_2\text{Si}_2\text{O}_7$ environmental barrier coatings to protect non-oxide silicon-based ceramics in gas turbines



UNIVERSITÄT  
BAYREUTH

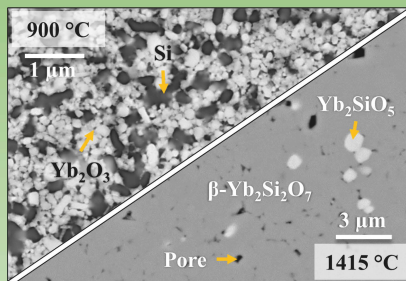


Schriftenreihe Keramische Werkstoffe  
Lehrstuhl Keramische Werkstoffe  
Herausgeber Prof. Dr.-Ing. Walter Krenkel

Band 16

Mateus Lenz Leite

*In situ* generated  $\beta\text{-Yb}_2\text{Si}_2\text{O}_7$  environmental  
barrier coatings to protect non-oxide  
silicon-based ceramics in gas turbines



Cuvillier Verlag Göttingen  
Internationaler wissenschaftlicher Fachverlag

<https://cuvillier.de/de/shop/publications/8609>

Copyright:

Cuvillier Verlag, Inhaberin Annette Jentzsch-Cuvillier, Nonnenstieg 8, 37075 Göttingen,  
Germany

Telefon: +49 (0)551 54724-0, E-Mail: [info@cuvillier.de](mailto:info@cuvillier.de), Website: <https://cuvillier.de>

## 1 Introduction and motivation

Over the last two centuries, economic growth has been driven at the expenses of the environment. In a scenario where the demand for energy constantly grows, fossil fuel-fired power generation still accounts for over 70% of the greenhouse gas emissions, caused mainly by the combustion of coal and oil. According to the International Energy Agency (iea), energy-related CO<sub>2</sub> emissions should be cut in half by 2050 compared to 2009 to limit the increase in the world average temperature by 2 °C. Despite the advances in renewable energy alternatives, their supply is strongly dependent on favorable weather conditions and their efficient storage is still difficult. Thus, the key factor for the transition towards a more sustainable future relies on decarbonizing power generation. Alone the substitution of heavy fossil fuels by natural gas is able to decrease the related emissions in approximately 50% [1–4]. Nevertheless, a developing interest has been shown for carbon-free fuel sources as ammonia and liquid hydrogen, which are potential alternatives to produce energy with a cleaner emission profile. However, the low heat of combustion and flammability of ammonia and the economically efficient storage and transport of liquid hydrogen still remain unsolved challenges for their sustainable utilization [5].

Besides the compactness, gas turbines can operate with versatile fuel sources and produce energy with high efficiency. For this reason, they have found increasing service in the past 60 years in the power industry both among utilities and industrial plants as well as for aviation throughout the world [6]. In combined cycle operation and with inlet temperatures exceeding 1400 °C, efficiencies as high as 63% can be achieved [2]. Therefore, different strategies are adopted to protect the currently used Ni-based superalloys such as the deposition of yttria-stabilized-zirconia thermal barrier coatings (TBC) and intensive film cooling. This standard is, however, not realistic when considering service for considerable amount of times ( $t > 10,000$  h), since the great mismatch between the coefficient of thermal expansion (CTE) of the TBC and the alloy increase the risk of coating spallation and limit the application of metal-based components in turbine engines [7–10]. Especially envisioning the use of carbon-free fuel sources in future gas turbines, water vapor is one of the main products of combustion, which intensifies the degradation of these alloys [5,11–13]. Hence, advances towards reduced greenhouse gas emissions and more efficient gas turbines require their substitution by more robust materials resistant to oxidation and corrosion, able to endure service at higher temperatures.

Due to the reduced density, lower CTE ( $3 - 5.5 \cdot 10^{-6} \text{ K}^{-1}$ ), high temperature creep resistance and melting points, non-oxide silicon-based ceramics as  $\text{Si}_3\text{N}_4$ , SiC and SiC/SiC composites stand out for application in combustion environments [14–21]. In oxidative environments, the formation of a thermally grown  $\text{SiO}_2$ -scale ensures a great oxidation stability. Nevertheless,  $\text{H}_2\text{O}_{(v)}$  reacts with this scale at temperatures above  $1200 \text{ }^\circ\text{C}$ , leading to corrosion and the rapid recession of the ceramic surface. Over the last three decades, progress has been made to develop reliable environmental barrier coatings (EBC) to hinder these detrimental effects [19,22–26]. Among the suitable EBC materials, rare-earth silicates have gained attention due to a high temperature endurance of at least  $1400 \text{ }^\circ\text{C}$  and very low  $\text{SiO}_2$  activity [10,19,27–29]. Despite the higher corrosion rates of the disilicates in comparison with monosilicates, the lower CTE results in a better thermomechanical compatibility to  $\text{Si}_3\text{N}_4$ , SiC and SiC/SiC substrates and should be considered when designing a reliable EBC for gas turbines. In special, ytterbium disilicate ( $\text{Yb}_2\text{Si}_2\text{O}_7$ ,  $\text{CTE} = 3.91 \cdot 10^{-6} \text{ K}^{-1}$ ) exhibits no polymorphic transition and is therefore an attractive EBC candidate [19,27,30,31].

Despite the suitable protection against corrosion, the diffusion of oxygen through the EBC during long-term service at high temperatures leads to the oxidation of the substrate and jeopardizes the mechanical stability of coated systems [32,33]. Therefore, thermomechanical compatible bond-coats based on mullite ( $\text{CTE} = 5.71 \cdot 10^{-6} \text{ K}^{-1}$ ) or silicon ( $\text{CTE} = 4.1 \cdot 10^{-6} \text{ K}^{-1}$ ) are applied [10,19,27,34–36]. In comparison with mullite, silicon bond-coats are dense and can effectively hinder the diffusion of oxygen by forming a slow-growing  $\text{SiO}_2$ -scale ( $\text{CTE} = 3.1 \cdot 10^{-6} \text{ K}^{-1}$ ,  $\beta$ -cristobalite). Moreover, they have been reported to enhance adhesion, whereas oxide coatings usually exhibit an insufficient bonding strength to non-oxide silicon-based ceramics [10,27,37].

The most common techniques for the deposition of EBC systems onto non-oxide silicon-based ceramics are plasma spray [10,27,34,38], chemical (CVD) [39,40] or physical vapor deposition (PVD) [20,24]. PVD and CVD techniques are usually denoted by the very low deposition rates ( $1 \mu\text{m h}^{-1}$ ), requiring extended processing times to achieve thick coatings [41]. The main disadvantages of plasma spraying lie within the evaporation of silica from the rare-earth silicate feedstock powder and in the rapid cooling rates during the coating deposition, resulting in an inhomogeneous phase composition and an amorphous microstructure. Due to the amorphous microstructure, plasma-sprayed coatings usually require a post-processing treatment at temperatures exceeding  $1200 \text{ }^\circ\text{C}$  and annealing times of over 24 h in air to enable phase crystallization [27,34]. Besides the energy and time-consuming procedures, another main drawback of the mentioned techniques is the difficult coating of complex geometries, as

required for gas turbines. In contrast, slurry-based techniques such as sol-gel or the polymer derived ceramics (PDC) enable the deposition of coatings by simple methods as spraying, spin- or dip-coating [42–46].

In special, the PDC route relies on the use of reactive silicon containing precursors as silazanes, carbosilanes and siloxanes. After or during the shaping process, a thermal treatment at low temperatures induces cross-linking, resulting in a thermoset, whereas further heating at above 400 °C yields a stable ceramic. Among the available precursors for coating application, silazanes stand out due to the commercial availability, high ceramic yield, strong adhesion to most substrates and high stability in oxidative and corrosive media [42,43,47]. Nevertheless, the protection of silazane-based coatings in such media often relies on the formation of a passivating SiO<sub>2</sub>-scale, which undergoes detrimental reaction with water vapor in combustion environments. Moreover, mass loss and densification during the polymer to ceramic transition cause a volume shrinkage exceeding 50% [42,48], limiting the applicable thickness of crack and pore-free coatings to only a few micrometers [49,50]. The adverse effects related to the precursor shrinkage can be overcome by the use of fillers, hence enabling the deposition of thicker coatings with tailored properties [43,48,49,51–53].

These fillers are usually classified as passive, active and meltable. In contrast to passive fillers, active fillers undergo reaction with the atmosphere, precursor or pyrolysis products, thus expanding in volume and yielding tailored ceramic phases. The main role of meltable fillers is to act as densifying agents during melting, sealing porosity and relaxing stresses due to CTE mismatches at high temperatures. Consequently, the deposition of dense coatings of up to 100 µm for protection of steel substrates against oxidation and corrosion up to 700 °C was achieved [51]. Moreover in previous work [54], it was demonstrated that silazanes react with rare-earth oxides (RE<sub>2</sub>O<sub>3</sub>, RE = Y or Yb) as active fillers during pyrolysis in air to yield the respective silicates according to Eq. 1.1.1 and 1.1.2. Due to the shrinkage of the silazane precursor during pyrolysis, crack-free but porous coatings could only be obtained by limiting its amount, whereas the deficit of silicon resulted in unconverted rare-earth oxides.



A similar coating strategy was reported for the generation of ytterbium mono- and disilicate coatings on Si<sub>3</sub>N<sub>4</sub> by the reaction of a polysiloxane and Yb<sub>2</sub>O<sub>3</sub> during pyrolysis. The Si<sub>3</sub>N<sub>4</sub> substrate was coated by dipping, followed by pyrolysis at 1000 °C in air and sintering at

1500 °C in N<sub>2</sub> atmosphere, achieving a coating thickness of 20 μm. However, no information about the formed crystalline phases was provided. Moreover, the coatings rapidly spalled-off during hot gas corrosion tests at 1450 °C for 200 h ( $p = 1 \text{ atm}$ ,  $p_{\text{H}_2\text{O}} = 0.18 \text{ atm}$  and  $v = 100 \text{ m s}^{-1}$ ) due to the residual porosity and insufficient adhesion to the substrate [55].

### 1.1 **Goals**

As mentioned before, ytterbium disilicate (Yb<sub>2</sub>Si<sub>2</sub>O<sub>7</sub>) is a very attractive material for the protection of non-oxide silicon-based ceramics in combustion environments due to the matching CTE, very low corrosion rate and no polymorphic crystalline transition. Plasma spraying, PVD and CVD are typical techniques for the deposition of EBCs, denoted by the energy and time-consuming procedures. By contrast, the PDC route stands out due to the low-cost and uncomplicated application of coatings by typical lacquer techniques based on reactive silicon-containing precursors. Despite the excellent adhesion and the proven potential of silazane-based coatings for protection of ceramic and metal substrates against oxidation and corrosion in harsh environments, the formation of SiO<sub>2</sub> limits their application in combustion environments. In this context, the conversion of forming SiO<sub>2</sub> into hot gas corrosion resistant phases like rare-earth silicates is imperative to increase the stability of silazane-based coatings.

As will be presented in Section 2.8, the high reactivity of silazanes with ytterbium oxide (Yb<sub>2</sub>O<sub>3</sub>) leads to the efficient formation ytterbium silicates upon pyrolysis in air. Nevertheless, monolithic samples based on this system are characterized by a high porosity content ( $\approx 40 \text{ vol}\%$ ) [54]. In addition, stable but porous coatings can only be achieved by limiting the fraction of silazane, which results in considerable amounts of unconverted ytterbium monosilicate (Yb<sub>2</sub>SiO<sub>5</sub>) and Yb<sub>2</sub>O<sub>3</sub> after pyrolysis. Due to the high CTE mismatch of these phases with non-oxide silicon-based ceramics, associated with the porous coating microstructure, only a limited protection against hot gas corrosion can be expected in combustion environments. Based on these premises and regarding the customary techniques for EBC application, the main goal of this work consisted in developing a straightforward and easier approach for the deposition of Yb<sub>2</sub>Si<sub>2</sub>O<sub>7</sub> coatings by the PDC route to hinder hot gas corrosion of non-oxide silicon-based ceramic components.

During the pyrolysis step of silazane-based coatings, their microstructure, composition and mechanical properties can be strongly influenced by the substrate. Therefore, the development of a slurry and the assessment of suitable pyrolysis parameters to yield dense and crystalline Yb<sub>2</sub>Si<sub>2</sub>O<sub>7</sub> should occur without the influence of a substrate by processing free-

standing samples as powder and monoliths. Subsequently, coating experiments should be carried out with a non-oxide silicon-based ceramic substrate (i.e.  $\text{Si}_3\text{N}_4$ , SiC or SiC/SiC). In order to enable a straightforward and easy coating application, the largest coating thickness should be obtained with the lowest number of steps to reduce the processing time. In addition, the influence of the selected substrate on the resulting coating properties should be investigated.

During service in gas turbines, water vapor is a main product of combustion, which composes approximately 10% of the atmosphere. Corrosion by water vapor at above 1200 °C and a flow velocity that can exceed 100 m s<sup>-1</sup> lead to the rapid volatilization of SiO<sub>2</sub> and the considerably high recession rates of ceramic components [11,15]. Besides hot gas corrosion, changes in the operating conditions of gas turbines such as starting or an emergency shut-down can cause harsh thermal shocks of more than 800 K within one second, leading to the evolution of additional thermal stresses [56], which must be endured by the coating system during the life expectancy of the components in gas turbines ( $t > 10,000$  h). During the evaluation of the performance of the coating system in turbine-like environments, it should remain well-adhered and reduce hot gas corrosion regarding uncoated substrates.

Since gas turbines are expected to operate for considerable amount of times and rare-earth silicate-based environmental barrier coatings are slowly corroded in hot gas environments, the deposition of thick coatings ( $> 100 \mu\text{m}$ ) is desired to extend the life span of coated ceramic parts. To obtain a coating system with high thickness, strong adhesion, low residual porosity and high thermomechanical stability are the greatest challenges of PDC processing, since most PDC-based coatings are limited to a few microns in thickness. Thus, alternatives should be sought to increase the achievable thickness of the PDC-based  $\text{Yb}_2\text{Si}_2\text{O}_7$  coating. At last, coating experiments should be carried out with other non-oxide silicon-based ceramics, followed by the characterization of the resulting microstructure and composition to evaluate the transferability of the developed coating technology.

## 2 State of the art

### 2.1 Overview about gas turbines

The gas turbine has found increasing service in the past 60 years in the power industry both among utilities and industrial plants as well as for aviation throughout the world. Its compactness, low weight, and multiple fuel application make it an attractive candidate for energy production. To the day, different commercially available gas turbines run on natural gas, diesel fuel, methane and vaporized fuel oils. Depending on the availability, natural gas is often the fuel of choice because of its clean burning and competitive price. Its low carbon-to-hydrogen ratio means that it emits substantially less CO<sub>2</sub> than other fossil fuels, which can reduce emissions in up to 50% compared to coal powered energy plants and does not require a post-combustion waste treatment [2,4,6]. Nevertheless, cleaner energy sources as liquid hydrogen and ammonia have gained increasing interest and are expected to be extensively used as fuel alternatives in the near future [5].

Due to their high flexibility, gas turbines are available in different sizes and power outputs ranging from 20 kW to 600 MW, which are among the most efficient types of heat engines. In simple cycle configuration, gross efficiencies ranging from 30 to 46% are usually achieved. However, by using the heat from the gas turbine exhaust to produce steam in a heat-recovery steam generator in combined cycle operation, the production of additional electrical power can lead to overall efficiencies that exceed 60%. The two factors, which most affect turbine efficiencies, are pressure ratios and temperature. The increase in the pressure ratio increases the overall efficiency at a given temperature. However, beyond a certain point at any given firing temperature, this may result in lowering the cycle efficiency. In contrast, for every 56 °C increase in the firing temperature, the work output increases approximately 8-13%, which results in a simple cycle efficiency increase of 2-4% [2,4,6].

For unprotected metal components, long-term service at temperatures above 704 °C leads to hot corrosion by salt melts contained in the used fuels. Anyhow, different strategies are adopted to protect the currently used Ni-based superalloys such as the deposition of yttria-stabilized-zirconia thermal barrier coatings (TBC) and intensive film cooling to keep the material temperature below 1050 °C. Due to the combination of both protection mechanisms, gas turbines can operate with firing temperatures up to 1427 °C, achieving an overall efficiency of 66% in combined cycle operation [7–10]. However, during starting up an operation or an emergency shut-down, the components in gas turbines may be subjected to a temperature gradient of above 800 K within one second, which leads to a tensile stress of several hundreds

of MPa and may cause the rapid spallation of the TBC due to the great mismatch between its coefficient of thermal expansion (CTE) with the alloy. These conditions can achieve an extreme point at the first stage of the gas turbine, where the gas flow velocity ( $265 \text{ m s}^{-1}$ ) and pressure (1.6 MPa) are high enough so that the heat transfer coefficient approaches that of a water quench [56,57].

The combustor, vanes and turbine blades constitute the most critical components in the hot section of existing high performance long-life gas turbines. The combustor and vanes operate at relatively high temperature and low stress conditions, whereas extreme conditions of stress and temperature can be expected to be faced by the turbine blades. In this case, the air flow velocity in combustors are generally limited to  $42 \text{ m s}^{-1}$  and the conditions of stress achieve about 35 MPa. In contrast, turbine blades are subjected to speed flows of over  $100 \text{ m s}^{-1}$  and stress conditions that can easily exceed 300 MPa [6,15,58]. Madhu [59] estimated the maximum stress of a gas turbine blade integrated disk of a jet engine achieved for different nickel-based superalloys (NI-90, MAR-M-247 and IN 718). Table 2.1.1 depicts a summary of the obtained results.

Table 2.1.1. Simulation of the maximum stress achieved for different Ni-based superalloys in jet engines, adapted from [59].

<b>Material</b>	<b>NI-90</b>	<b>MAR-M-247</b>	<b>IN 718</b>
RPM	29,000	29,000	29,000
Material temperature (°C)	725	725	725
Young's modulus at 725 °C (GPa)	153	171	157
Yield strength at 725 °C (MPa)	580	800	852
Ultimate tensile strength at 725 °C (MPa)	816	1002	933
Maximum achieved stress (MPa)	557	762	731

Besides these extreme conditions, thermal fatigue, oxidation, and corrosion also decrease the service life of the components in gas turbines. Especially the extreme conditions of stress, temperature and corrosion make the design of suitable materials for turbine blades a challenge. Materials characteristics in a turbine blade for high performance in the long-term include limited creep, high rupture strength, resistance to corrosion, good fatigue strength, low coefficient of thermal expansion and high thermal conductivity to reduce thermal strains [6,15,58]. Thus, due to the reduced density, low CTE ( $3 - 5.5 \cdot 10^{-6} \text{ K}^{-1}$ ), high temperature creep



resistance and melting points, non-oxide silicon-based ceramics as  $\text{Si}_3\text{N}_4$ , SiC and SiC/SiC composites stand out for application in combustion environments [14–21].

An increase in the operating temperature from 982 °C to 1371 °C by the use of uncooled ceramic blades provides an improvement in the fuel consumption of more than 20%, which implies that power almost doubles for the same engine size. In other words, the engine size could be reduced in half and still retain the same power output. Other advantages of ceramic materials are the good tolerance to fuel contaminants such as sodium and vanadium, which are present in low-cost fuels and are highly corrosive to currently used Ni-based superalloys. Besides that, ceramics are also over 50% lighter than the superalloys [6]. By the implementation of ceramic components in future gas turbines, operating temperatures that exceed 1500 °C are expected to be reached [10,56].

## **2.2 Non-oxide silicon-based ceramics**

The substitution of Ni-based superalloys by ceramic components in gas turbines accounts for higher efficiencies and lower emissions, besides the reduction in the turbine overall weight and size as detailed in Section 2.1. For the long-term service at temperatures of 1200 °C and above, only non-oxide silicon-based ceramics like silicon nitride ( $\text{Si}_3\text{N}_4$ ), silicon carbide (SiC) and fiber reinforced silicon carbide matrix composites (SiC/SiC) are suitable [14–21]. In comparison with SiC,  $\text{Si}_3\text{N}_4$  stands out due to the higher fracture toughness caused by the formation of needle-like  $\beta$ - $\text{Si}_3\text{N}_4$  crystals from  $\alpha$ - $\text{Si}_3\text{N}_4$  during sintering, capable of deflecting cracks. However, due to the brittle behavior of monolithic ceramics, their application is rather meaningful as structural components for stationary gas turbines. In non-stationary turbines as aircraft engines, additional problems may occur such as the foreign object damage (FOD) or strong vibration, which require an even higher fracture toughness and damage tolerance. For this purpose, only non-oxide ceramic matrix composites (CMCs) as SiC/SiC are suitable [60–62]. In this section, a summary of the processing routes and resulting properties of the different  $\text{Si}_3\text{N}_4$  and SiC ceramics and SiC/SiC composite will be given.

### ***2.2.1 Silicon nitride ( $\text{Si}_3\text{N}_4$ )***

In comparison with other high-performance ceramics,  $\text{Si}_3\text{N}_4$  stands out due to the combination of good mechanical properties at room and high temperatures. Owing to the strong covalent nature of the Si-N bonds of  $\text{Si}_3\text{N}_4$ , its sintering through a solid-state reaction is

practically impossible. At ambient pressure, this ceramic has no melting point, however it starts decomposing at a temperature of 1877 °C. Two processing routes are usually adopted for the processing of Si<sub>3</sub>N<sub>4</sub> ceramics. The first one consists of nitriding elemental Si, hence leading to the formation of Si<sub>3</sub>N<sub>4</sub>, which is named as reaction bonded silicon nitride (RBSN). The advantage of this method is the low volumetric shrinkage of less than 1%. Anyhow, a residual porosity of 10 to 30 vol% is usually obtained, which is associated with a low fracture toughness of less than 400 MPa. The second method and more efficient to obtain dense ceramic bodies consists of mixing 1 μm Si<sub>3</sub>N<sub>4</sub> powders with additives, followed by sintering, commonly classified as pressureless sintering (SSN, up to 0.1 MPa), gas pressure sintering (GPSN, up to 10 MPa), hot isostatic pressing (HIPSN, up to 200 MPa) and hot-pressing (HPSN).

The most commonly used sintering additives consist of binary oxides like Y<sub>2</sub>O<sub>3</sub>, rare-earth oxides, Al<sub>2</sub>O<sub>3</sub> and MgO. During heating of the processed green body, the reaction of these oxides with SiO<sub>2</sub> available at the surface of the Si<sub>3</sub>N<sub>4</sub> feedstock powder forms silicate melts, which densify the microstructure of Si<sub>3</sub>N<sub>4</sub>. This causes the solubilisation of the α-Si<sub>3</sub>N<sub>4</sub> phase and its precipitation as β-Si<sub>3</sub>N<sub>4</sub>. Due to the hexagonal crystalline structure, the β-Si<sub>3</sub>N<sub>4</sub> phase is known by its needle-like crystals and is often referred to as an *in situ* reinforcement. After sintering, most sintering additive systems form an amorphous or semi-crystalline grain boundary phase. The mechanical properties of Si<sub>3</sub>N<sub>4</sub> are usually dependent on the raw materials, sintering additive content and their composition, as well as the processing route. The density varies according to the employed sintering additive system, usually lying between 3.2 and 3.6 g cm<sup>-3</sup>. In addition, a good thermal shock resistance is reported due to the low CTEs of approximately 3 to 3.2 10<sup>-6</sup> K<sup>-1</sup> and the presence of the β-Si<sub>3</sub>N<sub>4</sub> phase. The most important mechanical properties of the different Si<sub>3</sub>N<sub>4</sub> ceramics according to the processing route are listed in Table 2.2.1 [61].

Table 2.2.1. Common properties of Si<sub>3</sub>N<sub>4</sub> materials according to the processing route [61].

Type	Young's modulus (GPa)	Flexural strength (RT, MPa)	Flexural strength (1400 °C, MPa)	Fracture toughness (MPa m <sup>1/2</sup> )
SSN	310 - 320	600 - 1000	100 - 300	5 - 7
GPSN	310 - 320	800 - 1300	100 - 300	5 - 10
HIPSN	310 - 320	800 - 1500	200 - 400	5 - 7
HPSN	310 - 320	1000 - 1700	200 - 400	5 - 7
RBSN	100 - 150	200 - 400	200 - 400	2 - 3

Despite the good mechanical properties at room temperature, a notorious decrease in the flexural strength at high temperatures is directly correlated to the softening of the amorphous grain boundary phase. Nevertheless, the crystallization of the grain boundary phase with an additional thermal handling in air at above 1000 °C improves the high temperature properties due to the reduced amount of low viscosity phases [63].

### 2.2.2 Silicon carbide (SiC)

Besides Si<sub>3</sub>N<sub>4</sub>, silicon carbide also stands out for high temperature application. Attractive properties of this ceramic are for example the high hardness, high temperature flexural strength and high thermal conductivity. Similarly to Si<sub>3</sub>N<sub>4</sub>, the sintering of SiC is extremely difficult and usually requires temperatures above 1900 °C, depending on the selected processing route. Some common processing routes are for example the pressureless sintering (SiC), liquid phase sintering (LPSiC), hot-pressing (HPSiC), hot isostatic pressing (HIPSiC) and silicon infiltration (SiSiC). Besides SiSiC, the sintering of SiC is achieved through the use of Al, B, C and their respective compounds like B<sub>4</sub>C, BN, AlB<sub>4</sub> or SiB<sub>6</sub> as sintering additives. In comparison with Si<sub>3</sub>N<sub>4</sub>, the higher decomposition temperature of SiC at above 2500 °C enables its sintering with a lower additive content ranging from approximately 0.2 to 3 wt% [61,64,65].

At temperatures above 2100 °C, the low temperature phase β-SiC transforms into α-SiC, which is accompanied by a grain growth, desired for *in situ* reinforcement properties. In comparison with the other sintering techniques, silicon infiltration enables the sintering of SiC at relatively low temperatures due to the melting and infiltration of the microstructure by Si or Si-based alloys at around 1414 °C, also limiting its application to this temperature due to the residual amount of Si. Depending on the sintering method, different densities (3.12 to 3.21 g cm<sup>-3</sup>) and CTE<sub>α<sub>30/1500</sub></sub> (3.60 - 4.9 10<sup>-6</sup> K<sup>-1</sup>) are reported as well as different grain boundary compositions, which influence directly the mechanical properties of SiC [61]. Table 2.2.2 summarizes the mechanical properties of SiC ceramics obtained by some of the common sintering methods.

Table 2.2.2. Common properties of SiC materials according to the processing route [61].

Type	Young's modulus (GPa)	Flexural strength (RT, MPa)	Flexural strength (1400 °C, MPa)	Fracture toughness (MPa m <sup>1/2</sup> )
SiSiC	400	350 - 370	200	3 - 4.7
SSiC	410	430	450	2.5 - 4.7